Vol 18 No 12, December 2009
1674-1056/2009/18(12)/5249-10

Chinese Physics B

© 2009 Chin. Phys. Soc.
and IOP Publishing Ltd

Complex network analysis in inclined oil–water two-phase flow*

Gao Zhong-Ke(高忠科) and Jin Ning-De(金宁德)†

School of Electrical Engineering and Automation, Tianjin University, Tianjin 300072*, China*

(Received 30 March 2009; revised manuscript received 11 May 2009)

Complex networks have established themselves in recent years as being particularly suitable and flexible for representing and modelling many complex natural and artificial systems. Oil–water two-phase flow is one of the most complex systems. In this paper, we use complex networks to study the inclined oil–water two-phase flow. Two different complex network construction methods are proposed to build two types of networks, i.e. the flow pattern complex network (FPCN) and fluid dynamic complex network (FDCN). Through detecting the community structure of FPCN by the community-detection algorithm based on K-means clustering, useful and interesting results are found which can be used for identifying three inclined oil–water flow patterns. To investigate the dynamic characteristics of the inclined oil–water two-phase flow, we construct 48 FDCNs under different flow conditions, and find that the power-law exponent and the network information entropy, which are sensitive to the flow pattern transition, can both characterize the nonlinear dynamics of the inclined oil–water two-phase flow. In this paper, from a new perspective, we not only introduce a complex network theory into the study of the oil–water two-phase flow but also indicate that the complex network may be a powerful tool for exploring nonlinear time series in practice.

Keywords: two-phase flow, complex networks, community structure, nonlinear dynamics
PACC: 0590, 0547, 4754

1. Introduction

The oil–water two-phase flow is commonly observed in wellbores, and its behaviour in a wide range of flow conditions and inclination angles constitutes a relevant unresolved issue for the petroleum industry. In the study of two-phase flow, flow patterns indicate how the phases are distributed and mixed due to the physical nature of the system. Two-phase flow patterns depend on the type of fluid–fluid combination, the flow rate and direction, the conduit shape, size and inclination. Further, heat and mass transfer rates, momentum loss, rate of back mixing and pipe vibration all vary greatly with the flow pattern. Hence, it is quite important and necessary to discern the flow patterns and study the nonlinear dynamics in different flow patterns. The first significantly important study on oil–water two-phase flow in inclined pipes was conducted by Hill and Oolman.[1] In an essentially qualitative study, Hill and Oolman experimentally investigated oil–water flow pattern behaviour and its effect on production logging instruments. Vigneaux *et al*[2] measured oil–water flow structure and provided a very good description of the flow phenomena for oil dispersed systems. Flores *et al*[3] presented a comprehensive study of oil–water two-phase flow patterns in vertical and inclined pipes of an inner diameter of 5.08 cm. Lucas and Jin[4,5] investigated the drift velocity model for inclined oil–water two-phase flow and found that the values for the distribution parameter and single-droplet terminal rise velocity (which are both required by the drift velocity model) were closely related to the inclination angle.

Influenced by many complex factors, such as fluid turbulence, phase interfacial interaction, local relative movement between phases and the existence of a gravitational component normal to the flow direction, the inclined oil–water flow presents a highly irregular, random and unsteady flow structure. Due to the complex nature of inclined oil–water two-phase flow, theoretical analyses have not been able to describe the system perfectly. Therefore, a new method is strongly required, whether experimentally or theoretically, to detect and describe the flow patterns in conditions near pattern transitions and the nonlinear dynamics in different flow patterns.

Meanwhile, the past few years have witnessed dramatic advances in the field of complex networks since the publication of the seminal studies of Watts and

*Project supported by the National Natural Science Foundation of China (Grant Nos 50674070 and 60374041), and the National High Technology Research and Development Program of China (Grant No 2007AA06Z231).
†Corresponding author. E-mail: ndjin@tju.edu.cn

Strogatz[6] as well as Barabási and Albert.[7] Complex networks, which have been observed to arise naturally in a vast range of physical phenomena, can describe any complex system that contains massive units (or subsystems) with nodes representing the component units and edges serving as the interactions between them. A lot of complex systems have been examined from the viewpoint of complex networks. Examples include World Wide Web,[8] metabolic networks,[9] protein networks in the cell,[10] gas-liquid flow pattern complex network,[11] traffic networks,[12,13] collaboration networks,[14] brain network[15] and earthquake networks.[16] These empirical studies have inspired researchers to develop a variety of techniques and models to help one understand or predict the behaviour of complex systems.[17−24] Complex networks, which provide us with a new viewpoint and an effective tool for understanding a complex system from the relations between the elements in a global way, not only may be a powerful tool for revealing information embedded in time series,[25,26] but also can be used to study nonlinear dynamic systems that cannot be perfectly described by theoretical model.

In this paper, we use complex networks to study the inclined oil–water two-phase flow. Two different network construction methods are proposed to build two types of networks, i.e. flow pattern complex network (FPCN) and fluid dynamic complex network (FDCN). We first construct the FPCN that contains 48 nodes by using a new method based on time-delay embedding and modularity, and we identify three typical inclined oil–water flow patterns by detecting the community structure of the resulting network. Then, in order to study the nonlinear dynamics of oil–water two-phase flow, we construct 48 FDCNs, each with 2000 nodes, under different flow conditions. Based on the investigation on the relevant statistical characteristics of the 48 resulting networks and two complexity measures (Lempel and Ziv complexity and approximate entropy), we finally find that power-law exponent and network information entropy, which are sensitive to the flow pattern transition, can both characterize the nonlinear dynamics of inclined oil–water two-phase flow. Using complex networks to analyse the characteristics of inclined oil–water two-phase flow measurement fluctuant signals could be useful exploration for revealing and understanding the flow pattern transition mechanism which cannot be described accurately by mathematical model because of the complexity and uncertainty it owns.

2. Flow pattern classification

The observed inclined oil–water flow patterns are water-dominated flows and transitionally flowing. The water-dominated flows include the dispersion of oil in water countercurrent flow and dispersion of oil in water pseudoslug flow. According to Flores *et al*,[3] the three typical flow patterns of inclined oil–water two-phase flow, observed in our experiment, can be categorized as follows (Fig.1).

Dispersion oil in water-countercurrent (D O/W CT) flow: The dispersion of oil in water countercurrent flow occurs at velocities of superficial oil and water velocities from low to moderate, in this flow pattern, the oil disperses in the continuous water as discrete, well rounded, droplets with sizes from mostly small to medium (see Fig.1(a)).

Dispersion oil in water-pseudoslugs (D O/W PS) flow: The dispersion of oil in water pseudoslug flow occurs at slightly higher superficial water velocities and for superficial oil velocities from low to moderate, in this flow pattern, the sequence of oil droplets observed in the countercurrent flow pattern is interrupted by water breaks, with the oil droplets grouping closer and forming packs at the top of the pipe (see Fig.1(b)).

Transitional flow (TF): The transitional flow occurs at moderate superficial oil velocities and for superficial water velocities from low to moderate, in this flow pattern, oil region forms at the topside of the pipe, at the bottom of the pipe exist just water with a few recirculating oil droplets, and in the middle region oil phase and water phase alternately appear as continual phase (see Fig.1(c)).

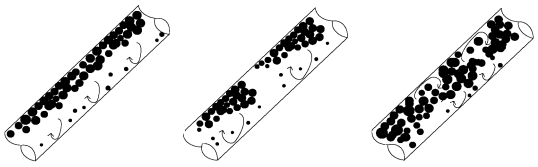


Fig.1. Three inclined oil–water flow pattern.

3. Experimental flow loop facility and data acquisition

The oil–water two-phase flow experiment in a 12.5-cm diameter pipe at an inclination angle of 45° from vertical was carried out in gas–oil–water three-phase flow laboratory of Tianjin University. The whole measurement system can be divided into several parts, including the VMEA (vertical multi-electrode array) conductance sensor that was designed and optimized by our research team (for further details, see Ref.[27]), exciting signals generating circuit, signal modulating module, data acquisition device and signal analysis software. The measurement circuit was embedded inside the instrument, and signals were transmitted to the data acquisition and processing system through cable connected outside the circuit system. The measurement system was excited by a 20-kHz constant voltage sine wave, and the value of exciting voltage is 1.4 V. The signal modulating module is mainly composed of three modules, which are differential amplifier, sensitive demodulation and low pass filter. The data acquisition equipment is selected from the National Instrument Company's product PXI 4472 data acquisition card, which is based on the PXI main bus technology, equipped with eight channels and synchronized acquiring function. The data processing part is realized through graphical programming language LABVIEW 7.1 wrapped in the data acquisition card, which can realize real time data waveform displaying, storing and analysing.

The experimental plan was like this. Let water flow into the pipe at a fixed flow rate, but let the oil flow in at a rate gradually increased, thereby changing the proportion of oil flow rate to water flow rate; for each proportion of oil flow rate to water flow rate, we acquired a conductance fluctuating signal from VMEA and observed a flow pattern variation, correspondingly. The water phase flow rate was between 0.0052 m/s and 0.3306 m/s, of which the oil phase was between 0.0057 m/s and 0.3306 m/s, and there were used 48 different proportions of oil flow rate to water flow rate in this experiment. The sampling frequency was 400 Hz, and the sampling data recording time for one measuring point was 60 s. We have acquired 48 conductance fluctuating signals in the experiment all told. The conductance fluctuating signals in three flow patterns measured from VMEA are shown in Fig.2, in which U_{SO} and U_{SW} represent oil superficial velocity and water superficial velocity, respectively.

Because of the significant difference in electrical sensibility between oil phase and water phase, the random flow of oil phase will cause voltage fluctuation on the measuring electrode under a certain sinusoidal input, which implies that the conductance fluctuating signals measured from the VMEA conductance sensor are related to the flow transition. Therefore, we construct complex networks from the conductance fluctuating signals and study the oil–water two-phase flow through analysing the resulting networks.

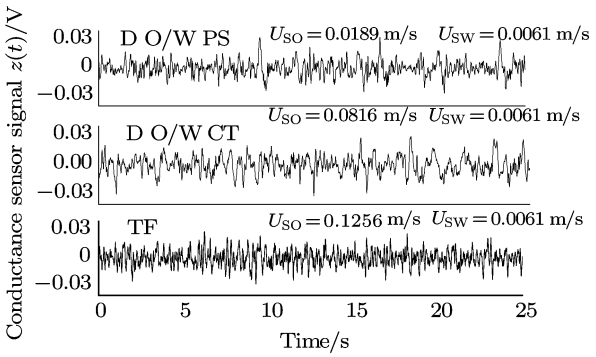


Fig.2. Conductance fluctuating signals in three inclined oil–water flow patterns.

4. Community structure versus flow pattern identification

4.1. Oil–water flow pattern complex network

Recently a new framework has been proposed to construct gas–liquid flow pattern complex network from signal time series (Gao Z K and Jin N D 2008 *Acta Phys. Sin.* **57** 6909). Essentially, this is a transformation from the two-phase flow to the complex network, which allows for the flow pattern identification to be studied via community structure of the network. In the present paper, we further construct an oil–water flow pattern complex network (FPCN) from the conductance fluctuating signals by considering each flow condition as a basic node and using the strength of correlation between nodes to determine network connection. Flow condition here means the flow behaviour under different proportions of oil flow rate to water flow rate in the pipe. Since we configured 48 different proportions of oil flow rate to water flow rate to obtain 48 conductance fluctuating signals in our oil–water two-phase flow experiment, there are 48 different flow conditions, i.e. the number of nodes contained in FPCN is 48.

We now briefly demonstrate how to construct an FPCN from time series based on the method of time delay embedding and modularity. Considering the nonlinear characteristics of the oil–water two-phase flow, we first use the method of time delay embedding[28] to process the conductance fluctuating signals. That is, we use C–C method[29] to calculate the values of delay time τ from the 48 conductance fluctuating signals, respectively, and from them choose an appropriate one that can make the FPCN modularity[30] largest. Then we extract six time-domain features and four frequency-domain features from each processed conductance fluctuating signal to form the characteristic vector. For each pair of characteristic vectors, $\boldsymbol{T}_i$ and $\boldsymbol{T}_j$, the correlation coefficient can be written as

$$C_{ij} = \frac{\sum\limits_{k=1}^{M} [\boldsymbol{T}_i(k) - \langle \boldsymbol{T}_i \rangle] \cdot [\boldsymbol{T}_j(k) - \langle \boldsymbol{T}_j \rangle]}{\sqrt{\sum\limits_{k=1}^{M} [\boldsymbol{T}_i(k) - \langle \boldsymbol{T}_i \rangle]^2} \cdot \sqrt{\sum\limits_{k=1}^{M} [\boldsymbol{T}_j(k) - \langle \boldsymbol{T}_j \rangle]^2}}, \tag{1}$$

where, M is the dimension of the characteristic vector, $\langle \boldsymbol{T}_i \rangle = \sum\limits_{k=1}^{M} \boldsymbol{T}_i(k) \Big/ M$, and $\langle \boldsymbol{T}_j \rangle = \sum\limits_{k=1}^{M} \boldsymbol{T}_j(k) \Big/ M$. C is a symmetric matrix and C_{ij} describes the state of connection between node i and j. Finally, choosing a critical threshold $r_{\rm c}$, the correlation matrix C can be converted into an adjacent matrix A, the rules of which read

$$A_{ij} = \begin{cases} 1, & (|C_{ij}| \geq r_{\rm c}), \\ 0, & (|C_{ij}| < r_{\rm c}), \end{cases} \tag{2}$$

that is, there will be an edge connecting node i and node j if $|C_{ij}| \geq r_{\rm c}$. On the other hand, there will not be an edge connecting node i and node j if $|C_{ij}| < r_{\rm c}$. Details about how to select an appropriate threshold and extract time-domain features can be seen in Ref.[11]. According to the principles we have put forward in Ref.[11], we choose $\tau = 9\Delta t$ (Δt is the sample interval of the conductance fluctuating signals) and $r_{\rm c} = 0.98$ to derive the oil–water FPCN.

It should be pointed out that, since the inclined oil–water two-phase flow is much more complex than gas-liquid two-phase flow, we in this study not only extract six time-domain features, just as what we have done in Ref.[11], but also extract four frequency-domain features to form the characteristic vector. The method of feature extraction in the frequency-domain was mainly referred to the way used by Darwich *et al*[31] which was based on the concept of linear prediction in speech signal processing.[32] The basic principle of this method is that the value of a signal point at present could be estimated by the linear combination of several previous points; the coefficient of this linear combination could be acquired when the deviation of the true value from the estimated value is minimum. The coefficients and the previous signals comprise a linear prediction model; the coefficients are called the orders of this model, which are also what we set as the frequency characteristic quantities. We assumed that the input Z_t could be expressed as follows:

$$Z_t = -\sum_{k=l}^{p} a_k Z_{t-k} + G \sum_{k=0}^{q} b_k U_{t-k} \quad (b_0 = 1), \tag{3}$$

where U_{t-k} are the unknown input signals, a_k ($1 \leq k \leq p$), b_k ($1 \leq k \leq q$) and G are all system parameters, of which G is the system gain, and a_k ($1 \leq k \leq p$), the coefficients of the linear combination, are just what we want as the frequency characteristic quantities. We choose the linear prediction model with four orders, which means we only need to figure out a_1, a_2, a_3 and a_4.

All the nodes and edges form the FPCN, and the topological structure of this network can be described with the adjacent matrix $\boldsymbol{A}$. The conditions $A_{ij} = 1$ and $A_{ij} = 0$ correspond to connection and disconnection, respectively.

4.2. Flow pattern identification based on community structure

After constructing the FPCN containing 48 nodes, we detect its community structure by using the community-detection algorithm based on K-means clustering, proposed in Ref.[11], and show in Fig.3

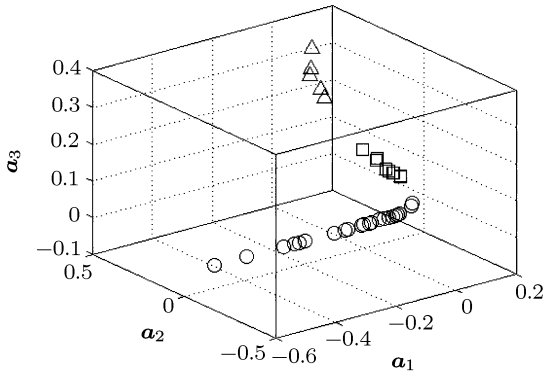


Fig.3. Components of the first non-trivial eigenvector $\boldsymbol{a}_1$ are plotted versus those of $\boldsymbol{a}_2$ and $\boldsymbol{a}_3$.

the distribution of the corresponding elements of the three first non-trivial eigenvectors. As can be seen, three different communities can be clearly identified when the components of the first non-trivial eigenvector $\boldsymbol{a}_1$ are plotted versus those of $\boldsymbol{a}_2$ and $\boldsymbol{a}_3$. The community structure of the FPCN, detected by community-detection algorithm based on K-means clustering, is shown in Fig.4. The community structure is drawn by the software "Ucinet" and "Netdraw".

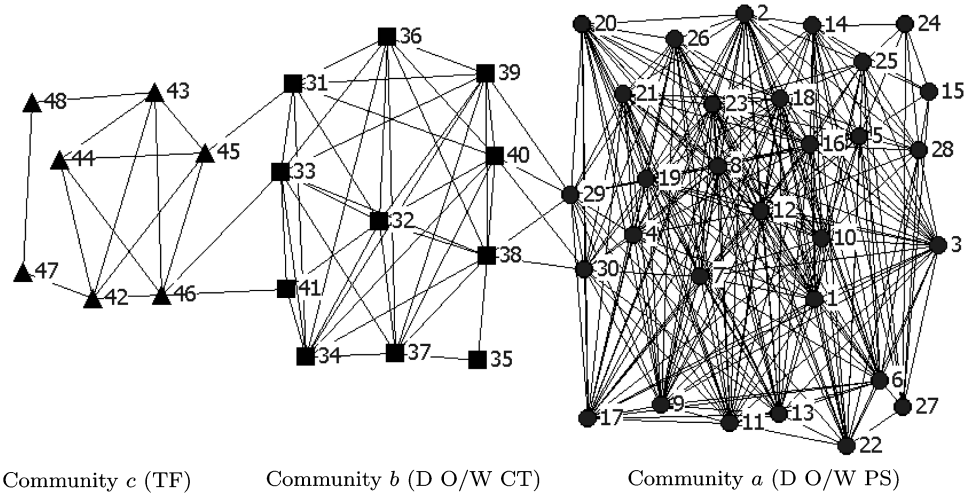


Fig.4. Community structure of the FPCN.

From the detected community structure, as shown in Fig.4, three communities of 30, 11 and 7 nodes are found, denoted as community a, community b and community c, respectively. Furthermore, combining with the experimental observations, we find that community a mainly corresponds to the dispersion oil in water-pseudoslugs (D O/W PS) flow, such as node 2 ($U_{\mathrm{SO}} = 0.0189$ m/s, $U_{\mathrm{SW}} = 0.0061$ m/s) and node 10 ($U_{\mathrm{SO}} = 0.0377$ m/s, $U_{\mathrm{SW}} = 0.0189$ m/s) both corresponding to D O/W PS flow; community b mainly corresponds to the dispersion oil in water-countercurrent (D O/W CT) flow, such as node 32 ($U_{\mathrm{SO}} = 0.0816$ m/s, $U_{\mathrm{SW}} = 0.0061$ m/s) and node 36 ($U_{\mathrm{SO}} = 0.2423$ m/s, $U_{\mathrm{SW}} = 0.0698$ m/s) both corresponding to D O/W CT flow; community c mainly corresponds to the transitional flow (TF), such as node 42 ($U_{\mathrm{SO}} = 0.1256$ m/s, $U_{\mathrm{SW}} = 0.0061$ m/s) and node 48 ($U_{\mathrm{SO}} = 0.2875$ m/s, $U_{\mathrm{SW}} = 0.0703$ m/s) both corresponding to transitional flow. Based on the community structure of flow pattern complex network, we also plot the oil–water flow pattern map (see Fig.5 for details) for a 12.5 cm diameter pipe at an inclination angle of 45°. Hence, through detecting the community structure of the FPCN, we have achieved the good identification of flow pattern in inclined oil–water two-phase flow by finding the three communities which correspond to the D O/W PS flow, D O/W CT flow and the transitional flow, respectively.

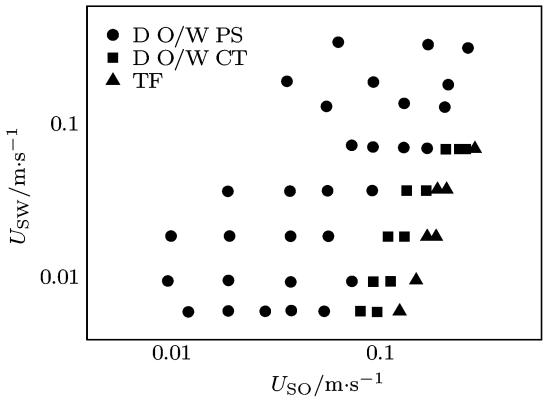


Fig.5. Oil–water flow pattern map for a 12.5-cm diameter pipe at an inclination angle of 45°.

5. Fluid dynamic complex network

To cast light on the nonlinear dynamics of inclined oil–water two-phase flow, we in this paper propose a new method of constructing fluid dynamic complex network (FDCN) from one conductance fluctuating signal, that is, we construct FDCN with each segment of signal time series represented by a single node and edge determined by the strength of correlation between segments. Considering a conductance fluctuating signal (i.e. a time series), denoted as $\{k_1, k_2, k_3, \dots, k_N\}$, we can obtain all the possible segments with length L, which read

$$\begin{aligned}
&\{\boldsymbol{S}_1 = (k_1, k_2, \dots, k_L)\}, \\
&\{\boldsymbol{S}_2 = (k_2, k_3, \dots, k_{L+1})\}, \\
&\{\boldsymbol{S}_3 = (k_3, k_4, \dots, k_{L+2})\}, \\
&\dots \\
&\{\boldsymbol{S_m} = (k_m, k_{m+1}, k_{m+2}, \dots, k_{m+L-1}) \,|m = 1, \dots, N - L + 1\}. \qquad (4)
\end{aligned}$$

For each pair of segments, $\boldsymbol{S}_i$ and $\boldsymbol{S}_j$, the correlation coefficient can be written as

$$C_{ij} = \frac{\sum_{k=1}^{L} [\boldsymbol{S}_i(k) \cdot \boldsymbol{S}_j(k)]}{\sqrt{\sum_{k=1}^{L} [\boldsymbol{S}_i(k)]^2} \cdot \sqrt{\sum_{k=1}^{L} [\boldsymbol{S}_j(k)]^2}}. \qquad (5)$$

Choosing critical threshold r_c, the correlation matrix $\boldsymbol{C}$ can be converted into adjacent matrix $\boldsymbol{A}$, of which the rules read $A_{ij} = 1$ if $|C_{ij}| \geq r_c$ and $A_{ij} = 0$ if $|C_{ij}| < r_c$.

Rho *et al*[33] considered the characteristics of the degree distribution functions for the constructed networks. At a special critical threshold the degree distribution will tend to obey a power law. The network at this transition point is used to detect non-trivial characteristics embedded in the autocorrelation matrix. Through the analysis of the evolution of FDCN containing 2000 nodes, we find that the resulting network can well keep the physically meaningful correlations when r_c is chosen as 0.95 (for details, see Fig.6).

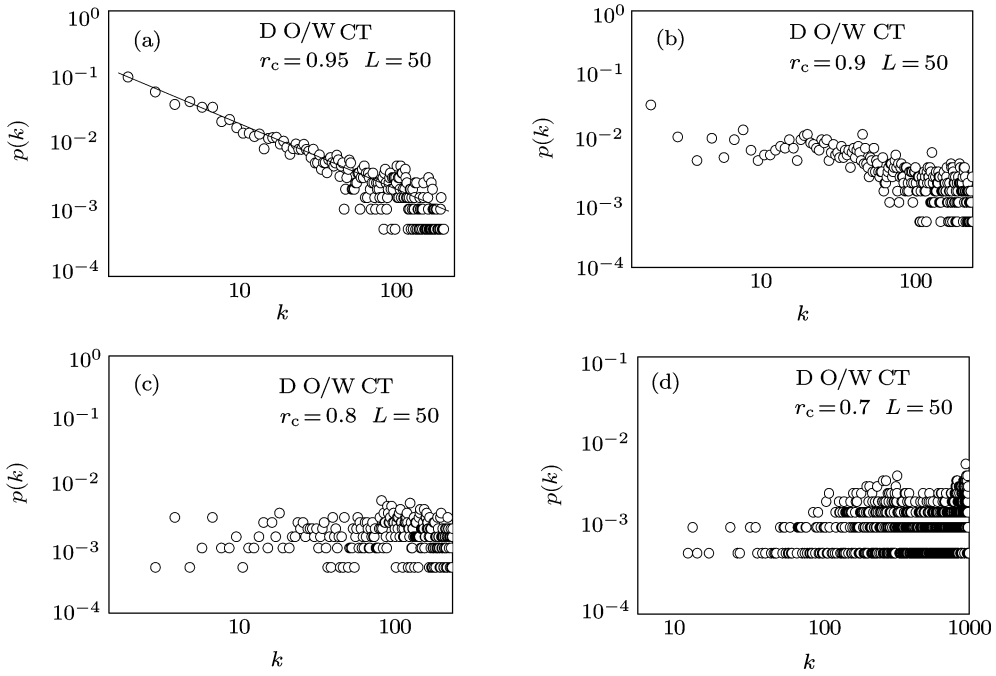


Fig.6. Evolution of the FDCN constructed with the conductance fluctuating signals of D O/W CT flow ($U_{SO} = 0.0816$ m/s, $U_{SW} = 0.0061$ m/s). When $r_c = 0.95$, the degree distribution obeys a power law. With the decrease of r_c, more and more edges are added, which may induce statistical fluctuations in the degree distribution. And finally, the power law is submerged in statistical noises.

The other adjustable parameter is the length of a segment, denoted as L. Short length will induce overestimated correlations. Increasing the length L can depress the finite-length-induced statistical fluctuations effectively. It should be long enough to give a reliable result. As shown in Fig.6, we find that when r_c and L are chosen as 0.95 and 50, respectively, the degree distribution of the resulting network can be well fitted to a power law as follows:

$$p(k) \sim k^{-\gamma}, \tag{6}$$

where the degree (or connectivity) k of a node is the number of edges incident with it, and the degree distribution $p(k)$ is defined as the probability that a node chosen uniformly at random has degree k; γ is the power-law exponent of degree distribution. In this study, we can expect a stability region of L, in which the resulting network can reveal the physically meaningful information embedded in the time series, that is, a proper L can be found just by simulating a special dynamical process of the complex network, i.e. changing the number of nodes and connections by increasing the value of L while keeping the power-law exponent of resulting network almost unchanged. By calculation, we plot the distributions of power-law exponent of different flow patterns in Fig.7.

From Fig.7, it is clear that the power-law exponent keeps stable when L ranges from 46 to 54. Hence, we choose $L = 50$ and $r_c = 0.95$ to derive the FDCN.

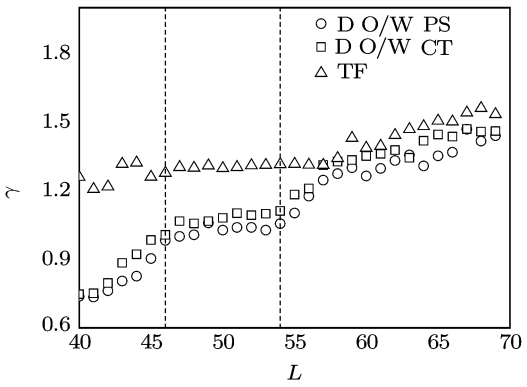


Fig.7. The power-law exponent distributions of three FDCNs with the change in segment length: D O/W PS flow ($U_{SO} = 0.0189$ m/s, $U_{SW} = 0.0061$ m/s), D O/W CT flow ($U_{SO} = 0.0816$ m/s, $U_{SW} = 0.0061$ m/s), and transitional flow ($U_{SO} = 0.1256$ m/s, $U_{SW} = 0.0061$ m/s).

6. Statistical characteristics versus nonlinear dynamics

6.1. Network degree distribution

By considering segments as nodes and associating network connectivity with the correlation among segments, time domain dynamics is naturally encoded into a network configuration. We select three types of flow pattern conductance fluctuating signals for constructing three FDCNs, each with 2000 nodes. After investigating the degree distribution of the three networks, we find their degree distributions can be well fitted to a power law, which indicates the scale-free property of the FDCN (for details, see Fig.8).

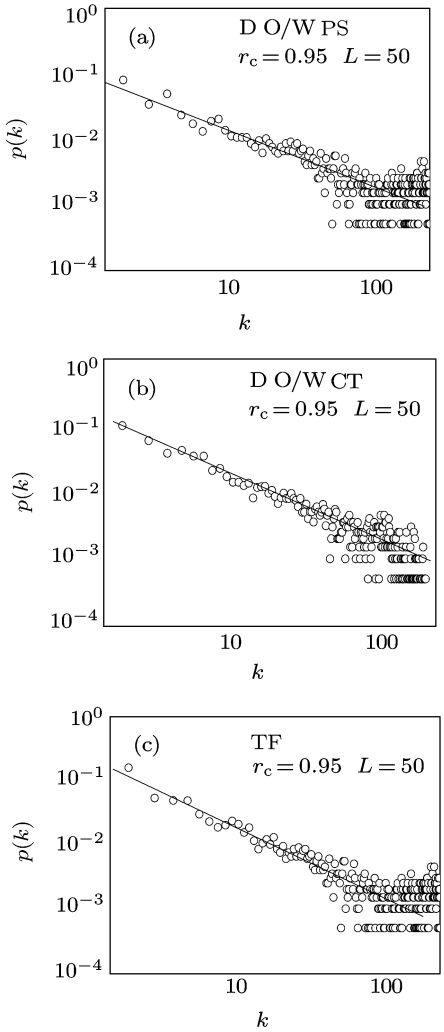


Fig.8. Degree distributions of different types of FDCNs: (a) D O/W PS flow ($U_{SO} = 0.0189$ m/s, $U_{SW} = 0.0061$ m/s), (b) D O/W CT flow ($U_{SO} = 0.0816$ m/s, $U_{SW} = 0.0061$ m/s), and (c) transitional flow ($U_{SO} = 0.1256$ m/s, $U_{SW} = 0.0061$ m/s).

To further explore the variations of the degree distribution power-law exponent in flow pattern transition, we construct 48 FDCNs under different flow conditions and calculate their corresponding power-law exponents. From Fig.9, we could see that the power-law exponents of D O/W PS flow are usually small and the power-law exponent increases as the flow pattern evolves from D O/W PS flow to D O/W CT flow. With the further increase of oil superficial velocity, the power-law exponent still increases as the flow pattern evolves from D O/W CT flow to transitional flow. $U_{\rm SO}$ and $U_{\rm SW}$, in Fig.9, represent oil superficial velocity and water superficial velocity, respectively.

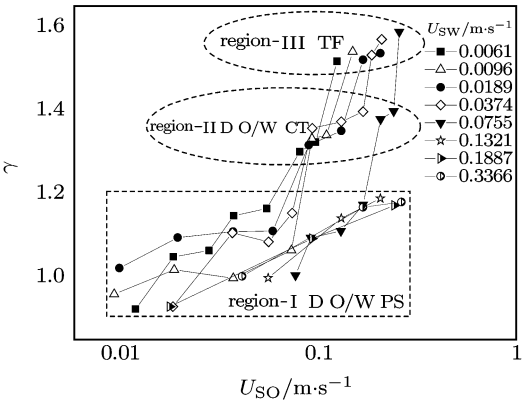


Fig.9. Power-law exponent distribution of 48 FDCNs with the increase of oil superficial velocity.

6.2. Network information entropy

The concept of Shannon's entropy[34] is a central role in information theory sometimes referred to as a measure of uncertainty. The entropy of a random variable is defined in terms of its probability distribution and can be shown to be a good measure of uncertainty. According to the definition of Shannon's entropy, we define a network information entropy for the FDCN and expect to investigate the nonlinear dynamics of oil–water flow through analysing the network information entropy.

Definition 1 Let $p(i)$ be the importance of node i

$$p(i) = k_i \Big/ \sum_{j=1}^{N} k_j, \tag{7}$$

where N is the number of nodes contained in the network; k_i (k_j) is the degree of node $i(j)$.

Definition 2 Let E be the network information entropy

$$E = -\sum_{i=1}^{N} k_{\rm B} p(i) \ln p(i), \tag{8}$$

where N is the number of nodes contained in the network and $k_{\rm B}$ is the Boltzmann constant. In order to simplify the calculation, here we let $k_B = 1$, that is,

$$E = -\sum_{i=1}^{N} p(i) \ln p(i). \tag{9}$$

Obviously, for a regular homogeneous network that contains N nodes, its network information entropy is the maximum, denoted as $E_{\max}$,

$$E_{\max} = -\sum_{i=1}^{N} \frac{1}{N} \ln \frac{1}{N} = \ln N. \tag{10}$$

On the contrary, for a star-shape network that has one core node with degree $N-1$ and any other node with degree 1, supposing $p(1) = 1/2$ and $p(i) = 1/2(N-1)(i \neq 1)$, its network information entropy is the minimum, denoted as $E_{\min}$

$$\begin{aligned} E_{\min} &= -\sum_{i=2}^{N} \frac{1}{2(N-1)} \ln \frac{1}{2(N-1)} - \frac{1}{2} \ln \frac{1}{2} \\ &= \frac{\ln 4(N-1)}{2}. \end{aligned} \tag{11}$$

In order to make the network information entropy not affected by the number of nodes contained in the network, we normalize E as follows:

$$\begin{aligned} E_N &= \frac{E - E_{\min}}{E - E_{\max}} \\ &= \frac{-2\sum\limits_{i=1}^{N} p(i) \ln p(i) - \ln 4(N-1)}{\ln N^2 - \ln 4(N-1)}. \end{aligned} \tag{12}$$

We calculate the network information entropy from the 48 constructed FDCNs. Figure 10 shows the variations of network information entropy with flow pattern changing. As can be seen, the network information entropy increases as the flow pattern evolves from D O/W PS flow to D O/W CT flow, and further increases as the flow pattern evolves from D O/W CT flow to transitional flow.

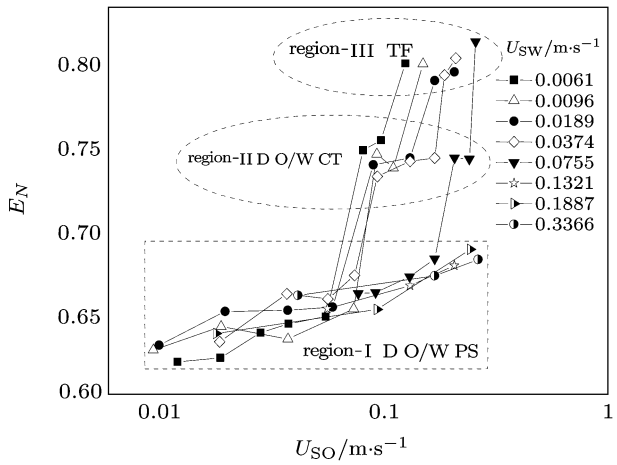


Fig.10. Network information entropy distributions of 48 FDCNs with the increase of oil superficial velocity.

6.3. Nonlinear dynamics of oil–water two-phase flow

Representing the conductance fluctuation signal through a corresponding FDCN, we can then explore the nonlinear dynamics of oil–water two-phase flow from network organization, which is quantified via a number of topological statistics. Through exploring the Lempel and Ziv complexity[35] and approximate entropy[36] of conductance fluctuation signals of oil–water two-phase flow, we show, in Fig.11 the variations of the two complexity measures with flow pattern changing. From Figs.9–11, we could see that there are good corresponding relations between complexity measures and the FDCN topological statistics (i.e. power-law exponent and network information entropy).

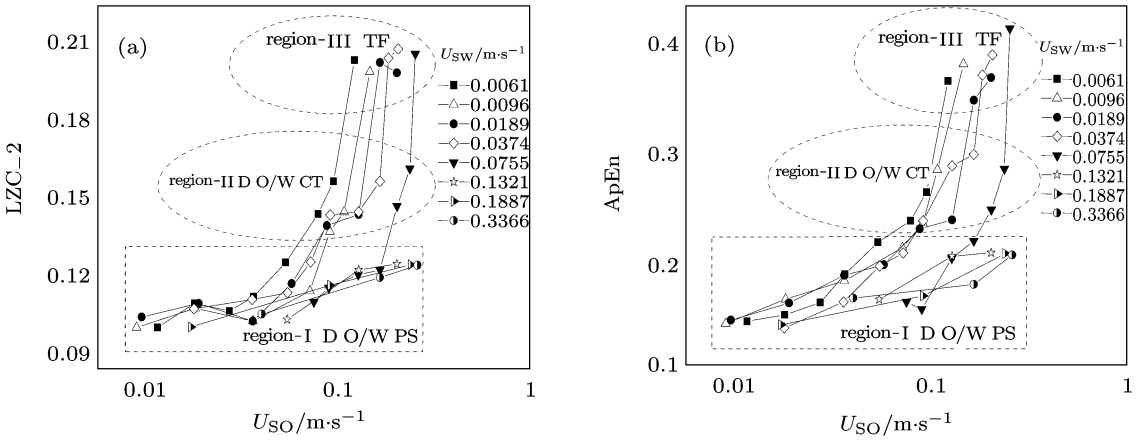


Fig.11. Complexity measure distributions with the increase of oil superficial velocity. Panel (a) shows Lempel and Ziv complexity and panel (b) displays approximate entropies.

The D O/W PS flow can be characterized by a sequence of pseudoslug units, and a pseudoslug unit consists of two major components, an oil pack and a trailing water break. At the front of the oil pack there is normally an oil globule, which is in most cases of elongated shape. The globule is followed by the pack itself, consisting of a large number of droplets with sizes ranging from small to medium. The oil pack is followed by a water break that carries at the top a very few slowly moving droplets left behind by the oil pack. Owing to the periodic alternating movements between oil plug and water plug, the dynamics in the D O/W PS flow is simple, corresponding to the small power-law exponent and network information entropy. When the oil superficial velocity is slightly higher, the D O/W CT flow appears, in which the oil disperses in the continuous water as discrete, well rounded droplets with sizes ranging from mostly small to medium. Because of the difference in density, the droplet flow occupies the upper regions of the pipe in an uninterrupted sequence of nearly uniform vertical spread. The outstanding characteristic of this flow pattern consists of local countercurrent flow of water, always at the bottom side of the pipe. And the countercurrent phenomenon is caused by the increase in magnitude of the gravitational component in the direction opposite to the main flow, which partially overcomes the linear momentum of the water phase. Because of the relative complex dynamics in D O/W CT flow, the power-law exponent and the

network information entropy increase as the flow pattern evolves from D O/W PS flow to D O/W CT flow. With the further increase of oil superficial velocity, the transitional flow (TF) appears in the region between the water-dominated flow patterns and oil-dominated flow patterns, and the dynamics of this flow becomes more complex than that of D O/W CT flow, corresponding to the further increase of the two network statistical characteristics as the flow pattern evolves from D O/W CT flow to transitional flow. Hence, the power-law exponent and the network information entropy, which are sensitive to the flow pattern transition, can both characterize the nonlinear dynamics of inclined oil–water two-phase flow.

7. Conclusions and discussions

We introduce complex network theory into the study of oil–water two-phase flow. Using a new method based on time-delay embedding and modularity, we construct FPCN from conductance fluctuating signals. Then we put forward a new flow pattern identification method of inclined oil–water two-phase flow by combining the community structure of FPCN.

In order to study the nonlinear dynamics of oil–water two-phase flow, 48 FDCNs under different flow conditions are constructed, and the nonlinear dynamics can then be studied by investigating the statistical characteristics of those networks. According to the investigation of the statistical characteristics of FDCNs, we confirm that the power-law exponent and network information entropy, which are sensitive to the flow pattern transition, can both characterize the nonlinear dynamics of oil–water two-phase flow.

The last decade has witnessed the birth of a new movement of interest and research in the study of complex networks, and the massive and comparative analysis of networks from different fields have produced a series of unexpected and dramatic results. With the study presented in this paper, a natural bridge between complex networks and oil–water two-phase flow has now been built. Further research on the self-organizing and self-evolution in these networks will help us establish a flow-evolution network model to explore the complex mechanism in two-phase flow.

References

[1] Hill A D and Oolman T 1982 *Journal of Petroleum Technology* **34** 2432

[2] Vigneaux P, Chenais P and Hulin J P 1988 *AIChE J.* **34** 781

[3] Flores J G, Chen X T, Sarica C and Brill J P 1999 *SPE Production and Facilities* **14** 102

[4] Lucas G P and Jin N D 2001a *Meas. Sci. Technol.* **12** 1546

[5] Lucas G P and Jin N D 2001b *Meas. Sci. Technol.* **12** 1529

[6] Watts D J and Strogatz S H 1998 *Nature* **393** 440

[7] Barabási A-L and Albert R 1999 *Science* **286** 509

[8] Albert R, Jeong H and Barabási A-L 1999 *Nature* **401** 130

[9] Jeong H, Tombor B, Albert R, Oltvai Z N and Barabási A-L 2000 *Nature* **407** 651

[10] Jeong H, Mason S, Barabási A-L and Oltvai Z N 2001 *Nature* **411** 41

[11] Gao Z K and Jin N D 2008 *Acta Phys. Sin.* **57** 6909 (in Chinese)

[12] Li X G, Gao Z Y, Li K P and Zhao X M 2007 *Phys. Rev.* E **76** 016110

[13] Chen Y Z, Fu C H, Chang H, Li N and He D R 2008 *Chin. Phys.* B **17** 3580

[14] Chang H, Su B B, Zhou Y P and He D R 2007 *Physica* A **383** 687

[15] Fang X L and Jiang Z L 2007 *Acta Phys. Sin.* **56** 7330 (in Chinese)

[16] Sumiyoshi A and Norikazu S 2006 *Phys. Rev.* E **74** 026113

[17] Nishikawa T, Motter A E, Lai Y C and Hoppensteadt F 2003 *Phys. Rev. Lett.* **91** 014101

[18] Pan Z F, Li X and Wang X F 2006 *Phys. Rev.* E **73** 056109

[19] Li K P and Gao Z Y 2007 *Chin. Phys.* **16** 2304

[20] Han X P, Zhou T and Wang B H 2008 *New Journal of Physics* **10** 73010

[21] Chen F, Chen Z Q and Yuan Z Z 2007 *Chin. Phys.* **16** 287

[22] Pei W D, Chen Z Q and Yuan Z Z 2008 *Chin. Phys.* B **17** 373

[23] Huang L, Lai Y C and Gatenby R A 2008 *Phys. Rev.* E **78** 45102(R)

[24] Yang R, Wang W X, Lai Y C and Chen G R 2009 *Phys. Rev.* E **79** 26112

[25] Luo F, Zhong J, Yang Y and Zhou J 2006 *Phys. Rev.* E **73** 31924

[26] Zhang J and Small M 2006 *Phys. Rev. Lett.* **96** 238701

[27] Jin N D, Zhao X, Wang Z Y, Jia X H and Chen W P 2008 *Meas. Sci. Technol.* **19** 045403

[28] Packard N H, Crutehfield J P and Farmer J D 1980 *Phys. Rev. Lett.* **45** 712

[29] Kim H S, Eykholt R and Salas J D 1999 *Physica* D **127** 48

[30] Newman M E J 2004 *Phys. Rev.* E **69** 066133

[31] Darwich T D, Toral H and Archer J S 1991 *SPE Production Engineering* **8** 265

[32] Makhoul H 1975 *Proc. IEEE* **63** 561

[33] Rho K, Jeong H and Kahng B 2006 *Physica* A **364** 557

[34] Shannon C E 1948 *Bell Syst. Tech. J.* **27** 379

[35] Lempel A and Ziv J 1976 *IEEE Trans. Inform. Theory* **22** 75

[36] Pincus S M 1991 *Proc. Nat. Acad. Sci. USA* **88** 2297